Volume 11, Issue 7, July – 2026 International Journal of Innovative Science and Research Technology
ISSN No:-2456-2165 https://doi.org/10.38124/ijisrt/26jul851

GIS-Based Spatio-Temporal Analysis of Vegetation Dynamics, Urban Expansion, and Land Surface Temperature in Davao City

Richelyn C. Dumdum[1]; Dr. Jason Ben R. Paragamac[2]

[2]EnP

[1,2]University of Mindanao, Professional Schools
[2]Marinduque State University

Publication Date: 2026/07/31

Abstract: The Earth's surface and atmosphere have been substantially modified by the growth of anthropogenic activities and urbanization. Changes in the composition and operation of the urban ecological system will affect the health of city dwellers by increasing the risk of heat exposure, increasing the risk of violence, illness, and mortality, and reducing labor productivity. Davao City is currently undergoing rapid urbanization, and no comprehensive study has examined the effects of the changes on vegetation indices, urban expansion, traffic density, and land surface temperature, which are likely to affect the area. This study analyzes the spatio-temporal change in vegetation indices, built-up expansion, traffic density, and land surface temperature from 2018 to 2022 using Landsat 8 imagery and GIS tools, particularly QGIS. The results show a moderate negative relationship between NDBI and NDVI ($r = -0.4313$), a strong positive relationship between NDBI and LST ($r = 0.6216$), and a weak negative relationship between NDVI and LST ($r = -0.2495$). Results highlight the interconnected influence of urbanization, vegetation dynamics, and thermal conditions within the study area, underscoring the need to integrate green infrastructure, particularly along major road networks, to mitigate rising land surface temperatures.

Keywords: *Vegetation Index, Urban Expansion, Land Surface Temperature, Spatiotemporal Correlation, Davao City, Philippines.*

How to Cite: Richelyn C. Dumdum; Dr. Jason Ben R. Paragamac (2026) GIS-Based Spatio-Temporal Analysis of Vegetation Dynamics, Urban Expansion, and Land Surface Temperature in Davao City. *International Journal of Innovative Science and Research Technology*, 11(7), 2112-2129. https://doi.org/10.38124/ijisrt/26jul851

I. INTRODUCTION

The Earth's surface and atmosphere have been substantially modified by growing anthropogenic activities and urbanization (Yao et al., 2017). Urbanization is a large-scale shift of population from rural to urban areas (Kuddus et al., 2020). Concurrently, the expansion rate of global urban land is double that of population growth (Angel et al., 2011). That number is expected to rise to more than 65% (United Nations, 2014), while less developed areas will hold 90% of this urban expansion (Fenta et al., 2017). However, the expanding population puts tremendous pressure on land expansion (Ray, 2011), and changes in land use alter the physical properties of land (Lai et al., 2016).

Among these effects is the urban heat island (UHI) (Peng et al., 2014), which is characterized by a temperature difference between urban and rural areas (Zhou et al., 2015) that resulted in a decrease in latent heat flux and the increase in sensible heat flux in urban areas (Imhoff et al., 2010). This issue of human-induced gravely impedes the numerous functions and services provided (Gessesse et al., 2015) as it threatens both the quality of air and water (Grimm et al., 2008), vegetation growth (Zhao et al., 2016), rainfall patterns (Chen et al., 2018) and climate (IPCC, 2014) which resulted in the increased demand for energy consumption (Cui et al., 2017), and decreasing net production (Chen et al., 2017) which can influence human life (Zhao et al., 2015).

The changes to the composition and operation of the urban ecological system will have an impact on the health of city dwellers (Fu et al., 2014) by raising the possibility of heat exposure that poses a health risk (Zhao et al., 2015) raising the chance of violence, illness, and mortality (Gong et al., 2012), and reduced labor productivity (Tong et al., 2021). It is anticipated that these effects will worsen due to global climate change (McCarthy et al., 2010). As urbanization continues (Yang et al., 2016), the sensitivity and level of exposure of individuals and communities

ISSN No:-2456-2165 https://doi.org/10.38124/ijisrt/26jul851

determine the type and extent of health concerns (Tong et al., 2021).

Traffic and urbanization are inextricably linked globally due to the growth and population of urban areas (Bertinelli & Black, 2004; Abbas, Selvanathan, & Selvanathan, 2023). Although traffic congestion has always been an important part of urban planning, the growing number of vehicles and demand for transportation have made it a significant problem that must be addressed (Gallivan & Heydecker, 1988), particularly with the growth of delivery and ridesharing services (Afrin & Yodo, 2020). Additionally, vehicles and cars are a contributing factor to urban heat emissions (Loiuza et al., 2015), which fuel urban smog and global warming (Wang et al., 2004; Watkins et al., 2007; Younger et al., 2008).

The expansion of transportation and industry increases the amount of greenhouse gases in the atmosphere, which in turn absorbs long-wavelength solar radiation from the earth and raises city temperatures (Grover & Singh, 2015), and the continuous constructions of buildings and roads (IPCC, 2019), pushing ecosystems and populations beyond their capacity to adapt increases with the severity of heat waves (Haines et al., 2019). Cities become warmer than their hinterlands and surroundings when there is a significant change in the land use/cover (LULC), which alters the energy balance (Grover & Singh, 2015) by replacing natural vegetation areas with impermeable surfaces like concrete, asphalt, and metal (Kuang et al., 2014) which seem to be the main factors causing the air to warm (Al Rakib et al., 2020).

The main factors contributing to heat intensification are surface parameters arising from manmade surfaces replacing wetlands, water surfaces, and vegetation cover, which lowers evapotranspiration and evaporation (Renard et al., 2019) and is further exacerbated by heat from air conditioners, factories, and cars, which warm the surrounding air (Liu & Zhang, 2011). An area's socioeconomic and natural resource conditions, as well as how they are used across time and location, are reflected in the state of its land use and land cover (Rawat & Kumar, 2015) and the reduction in the quantity of land covers or green spaces is the outcome of the increased in land usage (Ursu et al., 2019) due to the growing urban population (Ramachandra et al., 2018) which can be seen as metropolitan areas appear to have greater temperatures than the adjacent rural ones (Lieu et al., 2016).

Land cover and vegetation can effectively lower air temperatures (Kophim, 2013), thereby reducing fluxes and the amount of heat radiation emitted by structures, leading to variations in atmospheric temperature after dusk (Perini et al., 2014). Land cover change refers to changes in continuous land characteristics, such as vegetation type, soil conditions, and other factors (Patel et al., 2019). The geographic and temporal conditions of land use or land cover in a given region are crucial for understanding how human activities interact with the environment. (Etefa et al., 2018).

Rapid urbanization affects the structure and function of ecosystems. (Sun & Caldwell, 2015) The alteration of land cover is a significant problem (Akpoti et al., 2016), and this transformation is primarily the result of human activities (Tewabe, 2020). The degree and kinds of disturbances to land use and land cover have a significant impact (Caldwell et al., 2012), including the conversion of marshes into farms, grasslands into cities, and crops into orchards (Awotwi et al., 2015), and agricultural land and forestland (Kurowska et al., 2020) has been replaced with residential land use (Ng et al., 2015), causing cropland and rangeland production to fall on a global scale drastically (D'Odorico et al, 2012).

Determining the extent of human influence on the environment is made easier by evaluating changes in land use and cover (Chowdhury, 2020). The vegetation index is analyzed and examined to determine the degree of LULC change (Grover & Singh, 2015). A Geographic Information System (GIS), a type of digital technology, integrates hardware and software to analyze, store, and map geographical data (Chao et al., 2018) using a database of spatial properties (Kebur, 2021). By integrating together seemingly unrelated data, it can help individuals and organizations better understand spatial patterns and relationships (National Geographic, 2022) such as how urban growth is structured in relation to the pattern of land use (Handayani et al., 2018) as well as the urban thermal conditions may be detected and inverted which has made it possible to measure urban geothermal temperatures using remote sensing bands (Mao et al., 2016). The flexible framework offered by GIS enables the collection, storage, display, and analysis of the digital data required for change detection (Wu et al., 2006).

A megadiverse region has been defined as the Philippines based on its tropical forests and biodiverse ecosystems (Domingo & Manejar, 2018) however, like the rest of the world, the Philippines is rapidly becoming more urbanized and has a higher population density (World Bank, 2017) while majority are concentrated in the Metro Manila region (Purio et al., 2022). Davao City is one of the largest cities in Asia, with a total land area of 2443.61 km2 (Cabrera & Lee, 2022). Approximately 41% of the city's land area is designated as alienable and disposable, while nearly half is designated as forestland with established timberland. (Acioly et al, 2005) However, it is also classified as a highly urbanized city in the southern Philippines (Dumdumaya & Cabrera, 2023). In addition, there are several cultural, environmental, and economic challenges associated with the ongoing modification of natural habitat for industrial, agricultural, and urban development goals. (Hearne & Gamboa, 2008).

Davao City is currently rapidly urbanizing, and several changes in vegetation indices, urban expansion, traffic density, and land surface temperature are possible, affecting the area. Moreover, there is limited empirical evidence examining the statistical relationships among NDVI, NDBI, traffic density, and land surface temperature. Over multiple years to better understand how urbanization and transportation activities collectively influence the city's

ISSN No:-2456-2165 https://doi.org/10.38124/ijisrt/26jul851

thermal environment. Therefore, it is necessary to carry out this study. The research objective is to analyze the spatio-temporal relationships among vegetation cover, urban expansion, traffic density, and land surface temperature in Davao City from 2018-2022 using Geographic Information System (GIS) specifically this study aims to (i) analyze the spatio-temporal changes of the Davao City land cover from 2018 to 2022 using Normalized Difference Vegetation Index (NDVI); (ii) determine the urban expansion in Davao City from 2018-2022 through Normalized Difference Built-up Index (NDBI); (iii) assess the spatial and temporal distribution of land surface temperature (LST) from 2018-2022 and lastly, (iv) analyze the relationship between NDVI, NDBI, and AADT with land surface temperature (LST) in Davao City using Pearson-r correlation analysis.

The conceptual basis of this study is from the study (Rashid et al., 2022) Impact of Land Use Change and Urbanization on Urban Heat Island Effect in Narayanganj City, Bangladesh: A Remote Sensing-based Estimation. They study the impacts of urbanization on the trend of temperature rise and the degradation of the ecological environment over eight years before and after the establishment of Narayanganj City by using the Geographic Information System to estimate spatiotemporal changes of NDVI, NDBI, and LST to compute the changes in transition between the research intervals (2011-2019) using the Semi-Automatic Plugin tool. LST has been calculated using a land-use change map, vegetation coverage computed from the Normalized Difference Vegetation Index (NDVI), building coverage assessed using the Normalized Difference Built-up Index (NDBI), and the Urban Thermal Field Variance Index (UTFVI) for evaluating the ecological index. When classifying an unknown pixel, the MLC quantitatively evaluates the variance and covariance of the category spectral response patterns. Based on statistical parameters, it is considered one of the most accurate classifiers (Shalaby & Tateishi, 2007).

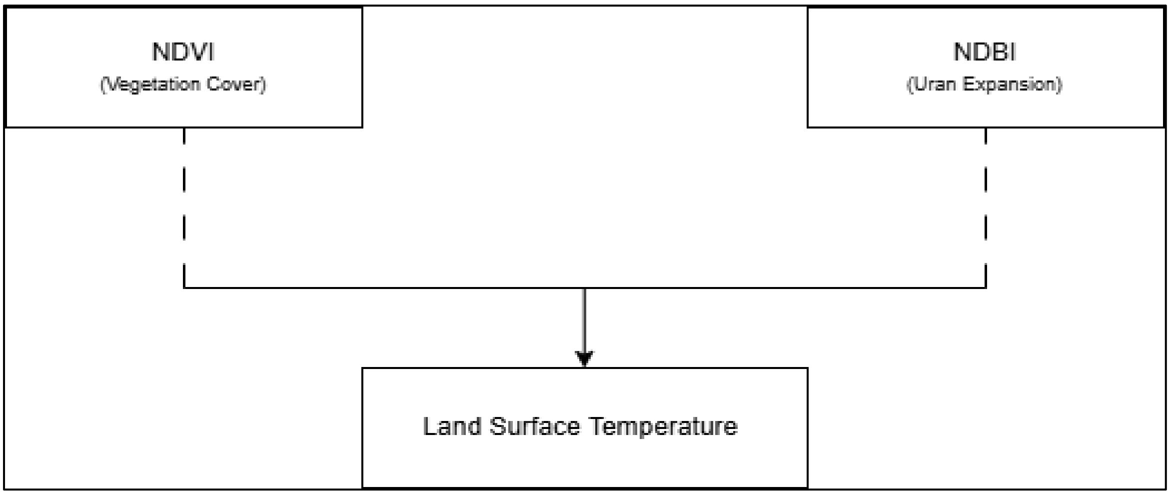

Fig 1 Conceptual Framework of the Study

II. MATERIALS AND METHODS

This chapter presents the materials and methods used to conduct the study, including the procedures for generating maps of vegetation dynamics, urban expansion, traffic density, and land surface temperature within the study area. It also described the statistical tool used for data analysis.

➢ *Research Design and Procedure*

The research design employed in the study were descriptive and quantitative non-experimental. A methodical process used to gather, examine, and present information regarding actual occurrences in order to characterize them in their natural setting (Stewart, 2024) which can examine one or more parameters using a variety of research techniques (McCombes, 2019). This involves the use of measurement tools and statistically represented data analysis (Mehrad et al., 2015) applied in natural sciences this approach employs mathematical, computational, and statistical methods to obtain and analyze complex data and numerical information (Surbhi, 2018). A research approach that involved assessing the region's physical attributes and examining analytical techniques using the Quantum Geographic Information System (QGIS). Landsat 8 satellite images from 2017, 2018, 2019, 2020, 2021 and 2022, with 10% cloud cover, were obtained from the United States Geological Survey (USGS) website. These datasets were standardized to a 30-meter cell size and unified to a common projection to facilitate spatial analysis. Pre-processing was conducted on all the satellite images, and QGIS will be utilized to carry out tasks related to changes in Normalized Difference Vegetation Index, Normalized Difference Built-up Index, and Land Surface Temperature (LST) computation.

➢ *Supervised Classification*

The Maximum Likelihood Classification method was used for image classification to quantitatively evaluate the variance and covariance of spectral response patterns across different categories when identifying an unknown pixel. Land cover change will be categorized into five distinct classes: Built-Up, including buildings, roads, construction sites, and industries. Dense Vegetation consisting of forest and mature tree cover. Moderate Vegetation encompasses all agricultural areas; Sparse vegetation includes arid lands, representing sands and exposed soils; and no vegetation, consisting of water bodies, covering waterlogged areas,

ISSN No:-2456-2165 https://doi.org/10.38124/ijisrt/26jul851

ponds, rivers, and lakes. This classification approach ensures accurate differentiation of land cover types based on their spectral characteristics.

- *Calculation of NDVI and NDBI*

After Landsat images will be classified, the Normalized Difference Vegetation Index (NDVI) is calculated based on the difference in reflectance between the near infrared (NIR) band and the red (RED) band of satellite imagery. The equation used for calculating NDVI is as follows:

$$NDBI = \frac{SWIR\ (Band\ 6) - NIR\ (Band\ 5)}{SWIR\ (Band\ 6) + NIR\ (Band\ 5)}$$

Where: NDVI values range from -1.0 to +1.0, where positive values represent areas with dense vegetation, while negative values indicate non-vegetated regions. In addition, for the Normalized Difference Built-up Index (NDBI) is used method for quantifying built-up land in urban areas. Built-up areas and bare soil are characterized by their reflectance in the Short-Wave InfraRed (SWIR) spectrum. The NDBI is calculated using the SWIR and Near-InfraRed (NIR) bands with this equation:

- *Calculation of LST and UTFVI*

In this study, several processes need to be followed due to the fact that the land surface temperature can only be obtained after the processes by applying all these steps in the raster calculator. First, is to calculate the top of Atmospheric (spectral radiance) to ensures the accurate measurement of radiant energy reaching the sensor, which reflects the surface's thermal properties with the following formula:

Where:

Calculation (Top of Atmospheric) spectral radiance.

$$TOA\ (L) = ML * Qcal + AL$$

ML = represents the band-specific multiplicative rescaling factor,
Qcal= is the Band 10 image,
AL = is the band-specific additive rescaling factor

Where:

Brightness Temperature BT:

$$BT = (K2 / (\ln (K1 / L) + 1)) - 273.15$$

K1 and K2= represent the thermal conversion constants specific to each band given in the satellite metadata (MTL.Text)

-273.15= the calculated temperature (in Kelvin) is adjusted by subtracting absolute zero

$$NDVI = NIR\ (Band\ 6) - R\ (Band\ 5) / NIR\ (Band\ 6) + R\ (Band\ 5)$$

Note: the calculation of the NDVI is important because, subsequently, the proportion of vegetation (Pv), which is highly related to the NDVI, and emissivity (ε), which is related to the Pv, must be calculated.

Where:

NIR=represents the near-infrared band (Band 6) R= represents the red band (Band5)

$$Pv = ((NDVI - NDVImin) / (NDVImax - NDVImin))$$

Note: the value of the NDVI depends on the calculated NDVI from the previous steps: PV= Proportion of Vegetation, NDVImin and NDVImax= can be obtain from the calculated NDVI from the previous steps

$$\varepsilon = 0.004 * Pv + 0.986$$

Where:

ε = Emissivity 0.004=constant Pv=Proportion of Vegetation 0.986= corresponds to a correction value of the equation

$$LST = (BT / (1 + (\lambda * BT / c2) * Ln(\varepsilon))$$

Finally apply the LST equation to obtain the surface temperature map.

Where:

BT: represents the brightness temperature λ: wavelength of emitted radiance
14388: constant
ε: emissivity

ISSN No:-2456-2165 https://doi.org/10.38124/ijisrt/26jul851

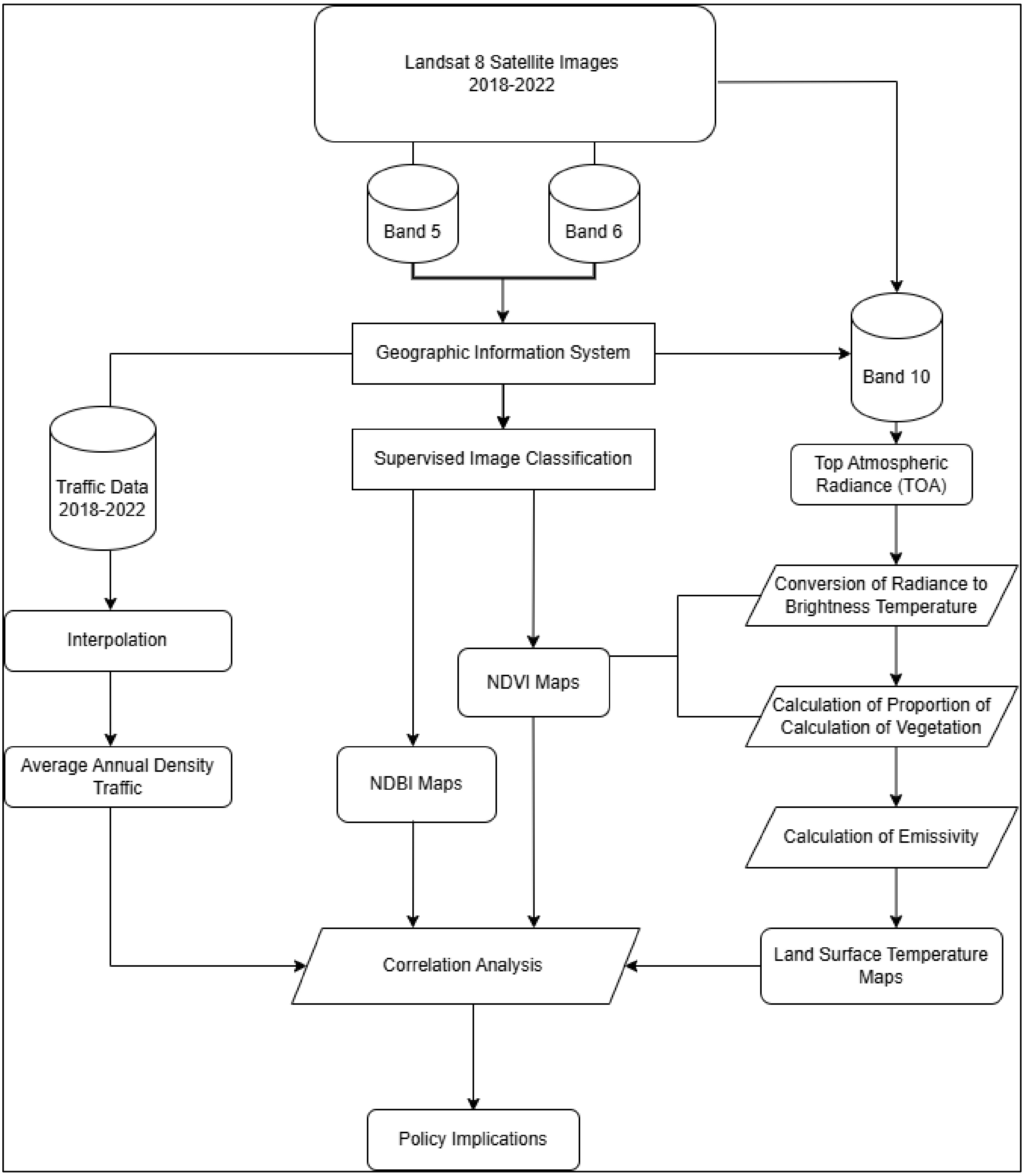

Fig 2 Methodological Framework of the Study

➢ *Study Area*

The study area, Davao City, located in the southeastern portion of Mindanao, lies within the coordinates of 7.1907° N latitude and 125.4553° E longitude (NAMRIA, 2023). Geographically, this region includes coastal plains, while other parts rise into mountains. The area is considered highly urbanized, with a population of 1,949,000 as of 2022 (PSA, 2022). Like many other cities, Davao City faces issues associated with urban heat islands, driven by factors such as the urban environment, a lack of vegetation, and poor planning (DCPO, 2022). Given this, it is crucial to study this region today due to the ongoing expansion of urban areas, the ongoing conversion of land cover to meet human needs, and the growing number of vehicles.

ISSN No:-2456-2165 https://doi.org/10.38124/ijisrt/26jul851

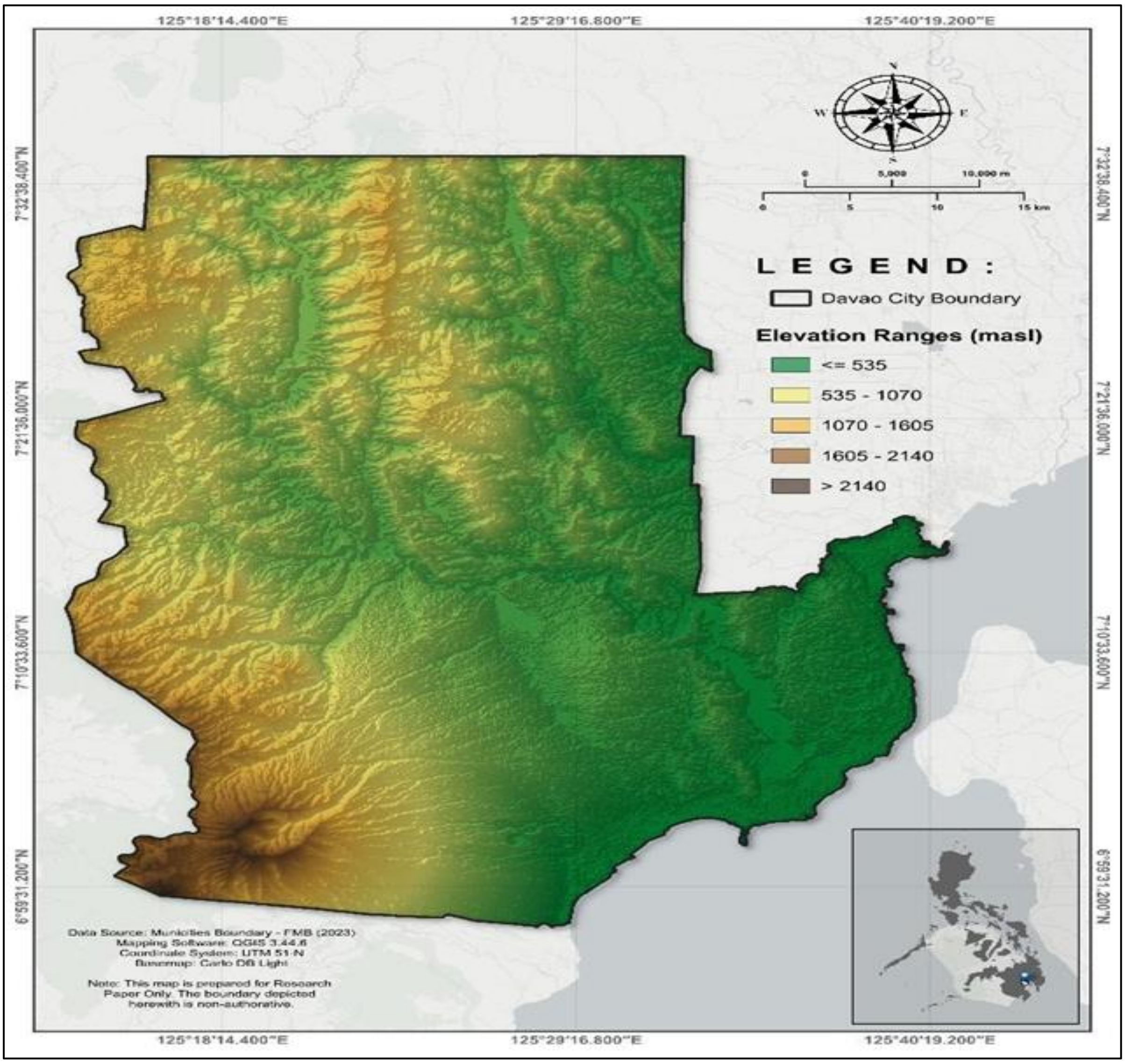

Fig 3 Map Showing the Location of the Study

III. RESULTS AND DISCUSSION

➢ *Vegetation Index in Davao City from 2018-2022*

Table 1 Vegetation Index of Davao City from 2018-2022

NDVI CLASSES	YEAR														
	2018			2019			2020			2021			2022		
	Area(ha)	%	%(/+)	Area(ha)	%	% (-/+)	Area(ha)	%	% (-/+)	Area(ha)	%	%(-/+)	Area(ha)	%	%(-/+)
No Vegetation	604.69	0.02		2044.53	0.08	238.11	2884.12	0.11	41.07	2157.59	0.09	-25.19	1964.26	0.08	-8.96
Built-up	42255.2	1.68		46288.32	1.84	9.54	73804.41	2.93	59.45	61893.36	2.46	-16.14	66322.65	2.63	7.16
Sparse Vegetation	386165.04	15.32		166834.06	6.62	-56.80	959445.89	38.07	475.09	225764.12	8.96	-76.47	197683.62	7.84	-12.44
Moderate Vegetation	999341.6	39.65		1641822.67	65.14	64.29	242273.5	9.61	-85.24	1670192.97	66.26	589.38	1796646.92	71.27	7.57
Dense Vegetation	1091924.92	43.32		663301.88	26.32	-39.25	1241883.54	49.27	87.23	560283.42	22.23	-54.88	457674.01	18.16	-18.31
TOTAL	2,520,291.46	100		2,520,291.46	100		2,520,291.46	100		2,520,291.46	100		2,520,291.46	100	

ISSN No:-2456-2165 https://doi.org/10.38124/ijisrt/26jul851

Table 1 and Figures 4 and 5 show the vegetation dynamics of Davao City from 2018 to 2022. The results show that notable variations were observed in the distribution of vegetation classes, reflecting changes in vegetation distribution. The lowest class, which corresponds to non-vegetated areas such as exposed soil and water bodies, accounted 0.08% (2,044.53 ha) of the total area in 2018, and increased marginally to 0.11% (2,884.12 ha) in 2019, increased in water bodies was largely driven by human activities, particularly the development of aquaculture ponds and water resource management (Jiang et al., 20024) which gradually decreased to 1, 964.26 ha (0.08%) by 2021, indicating that the non-vegetated class occupied only a small proportion of the area of study.

The built-up class similarly exhibited modest fluctuations, from 46,288.32 ha (1.84%) in 2018 to 73,804.41 ha (2.46%) in 2020, and increased slightly to 66,322.65 ha (2.63%) in 2021. Accelerating urbanization is a major driver of vegetation loss (Seto et al., 2012), reduction of areas essential for conserving biodiversity (Aronson et al., 2017), and More substantial variations were evident in the vegetation classes: sparse, moderate, and dense. For sparse vegetation, which expanded considerably from 166,834.06 ha (6.62%) in 2018 to 959,445.89 ha (38.07%) in 2019, and then decreased sharply to 225,764.12 ha (8.96%) in 2020, before increasing again in 2021. A similar decrease was also observed in the moderate vegetation class, which initially covered 1,641,822.67 ha (65.14%) in 2018 and dropped substantially to 242,273. 50 ha (9.61%) in 2019, which increased a year later to 1,670,192.97 ha (66.26%) in 2020 and further increased in 2021.

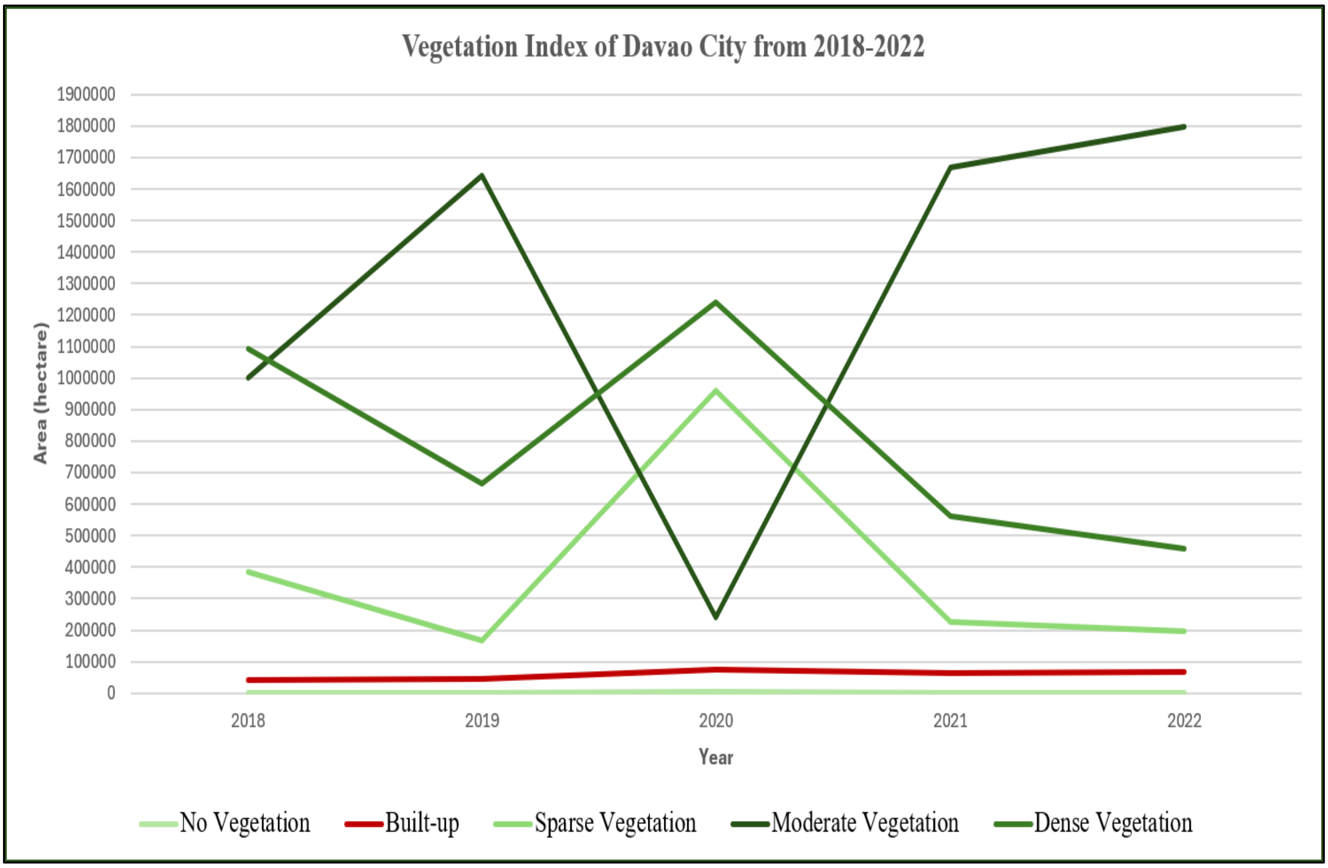

Fig 4 Graph Showing the Vegetation Index of Davao City from 2018-2022

Lastly, for the dense vegetation class represents healthy vegetation such as forest and mature tree cover expanded from 663, 301, 88 ha (26.32%) in 2018 to 1, 241, 833.54 ha (49. 27%) in 2019, but subsequently declined to 560, 283.42 ha (22.23%) in 2020 and 457, 674. 01 ha (18.16%) in 2021, this change in vegetation cover influenced vegetation phenology and environmental variability, as indicated by the values (Tucker, 1779; Jensen, 2015) and seasonal vegetation responses, as well as agricultural cycles (Pettorelli et al., 2005; Weng, 2012). This reduction in vegetation restricts ecosystem services such as carbon sequestration and flood control (Tzoulas et al., 2007), leading to flooding (Gunawaderna et al., 2017) and increased urban temperatures (Bowler et al., 2010).

ISSN No:-2456-2165 https://doi.org/10.38124/ijisrt/26jul851

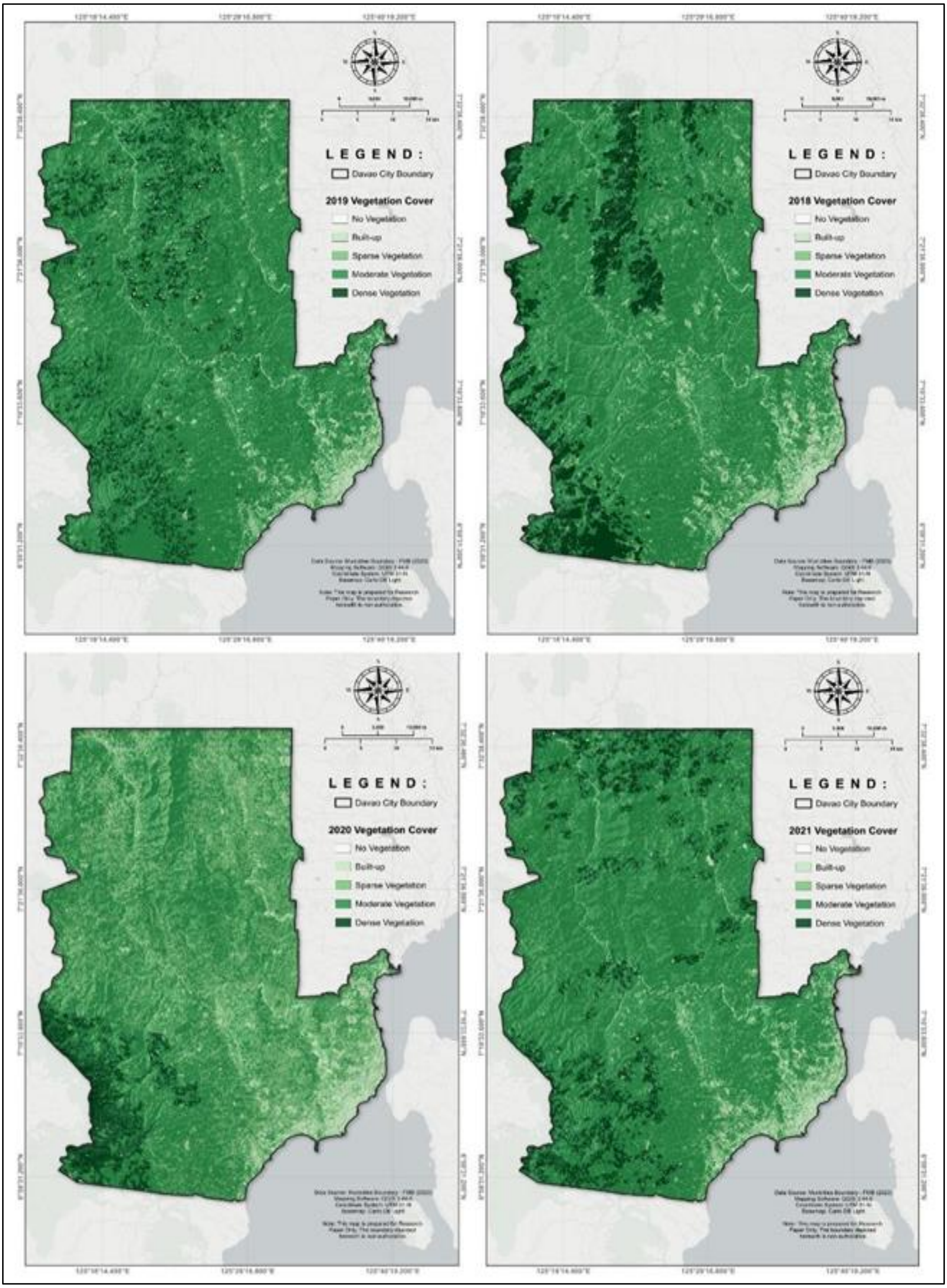

ISSN No:-2456-2165 https://doi.org/10.38124/ijisrt/26jul851

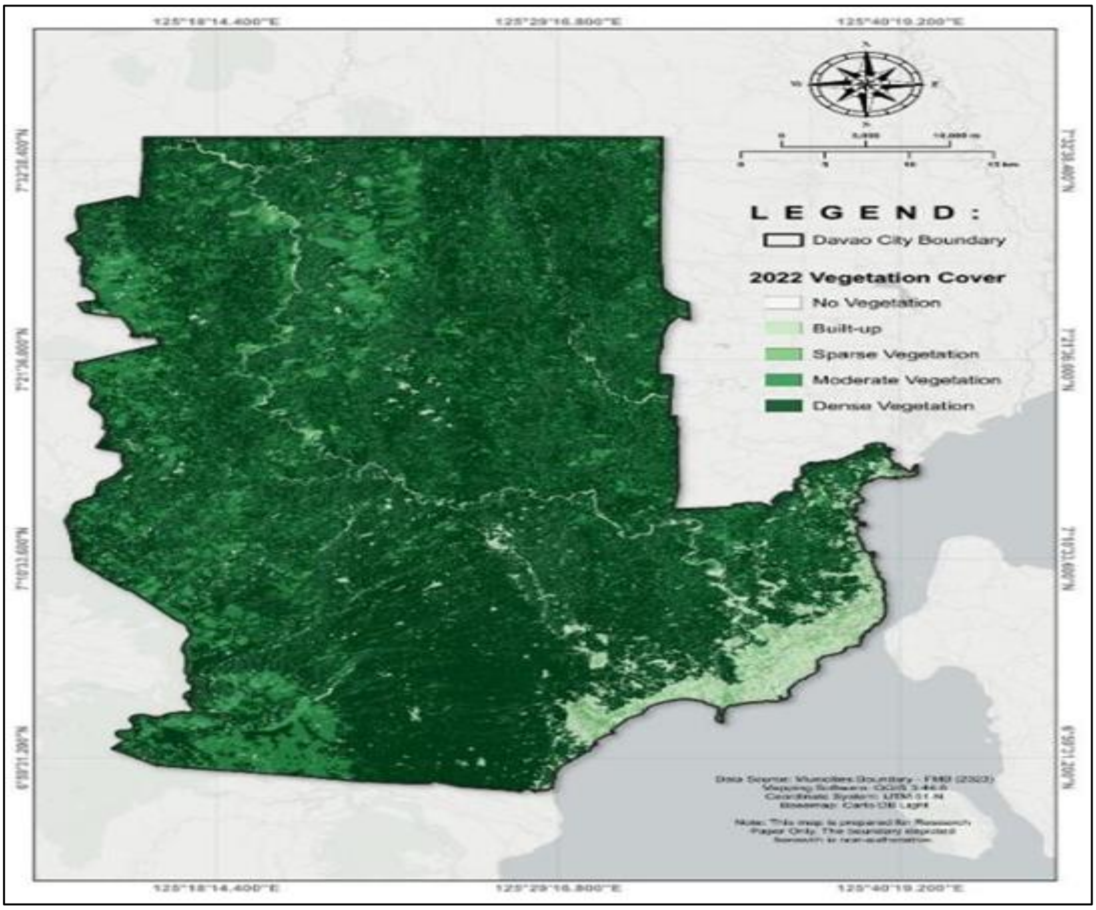

Fig 5 Spatio-Temporal Change in Vegetation Dynamics of Davao City from 2018-2022

➢ *Built-up Expansion Index of Davao City from 2018-2022*

Table 2 and Figures 6 and 7 present the built-up expansion results for Davao City during the 2018-2022 study period. The analysis shows noticeable variations in the spatial distribution of the identified land cover classes. Built-up and dense vegetation classes consistently occupied relatively small proportions of the study area cand exhibited considerable annual fluctuations, with built-up ranging from 8,009.92 ha (0.32%), which sharply decreased to 2, 135.94 ha (0.08%); however, it considerably increases by 7.941.21 ha (0.32%) In 2020, but declined to 5, 376.47 ha (0.07%) in 2021, and up to 2022. The relatively limited extent of built-up area suggested that urban expansion accounted for only a small proportion of urban surfaces (Zha et al., 2003; Weng, 2012).

Table 2 Built-up Index in Davao City from 2018-2022

NDBI CLASSES	YEAR														
	2018			2019			2020			2021			2022		
	Area(ha)	%	%(/+)	Area(ha)	%	% (-/+)	Area(ha)	%	% (-/+)	Area(ha)	%	%(-/+)	Area(ha)	%	%(-/+)
Dense Vegetation	61770.12	2.45		4237.17	0.17	-93.14	21502.75	0.85	407.48	1370.42	0.05	-93.63	6243.28	0.25	355.57
Moderate Vegetation	2046419.69	81.2		1850986.93	73.44	-9.55	1629795.75	64.66	-11.95	1723305.97	68.38	5.74	1858093.01	73.72	7.82
Sparse Vegetation	316523.51	12.56		559724.75	22.21	76.84	669415.58	26.56	19.60	655774.56	26.02	-2.04	552219.2	21.91	-15.79
Mixed Areas	87568.22	3.47		103206.66	4.1	17.86	191636.16	7.6	85.68	134464.01	5.34	-29.83	101996.87	4.05	-24.15
Built-up	8009.92	0.32		2135.94	0.08	-73.33	7941.21	0.32	271.79	5376.47	0.21	-32.30	1739.09	0.07	-67.65
TOTAL	2,520,291.46	100		2,520,291.46	100		2,520,291.46	100		2,520,291.46	100		2,520,291.46	100	

ISSN No:-2456-2165 https://doi.org/10.38124/ijisrt/26jul851

Moderate vegetation remained the predominant class, comprising 2,046,419.69 ha (81.20%) of the total area in 2018, decreased to 1,629,795.75 ha (64.66%) in 2020, and subsequently increased to 1,858,093.01 ha (73.72%). In contrast, sparse vegetation expanded from 316,523.51 ha (12.56%) in 2018 to 669,415.58 ha (26.56%) in 2020, then suddenly decreased to 552,219.20 ha (21.91%) in 2022, suggesting a change in vegetation density over time.

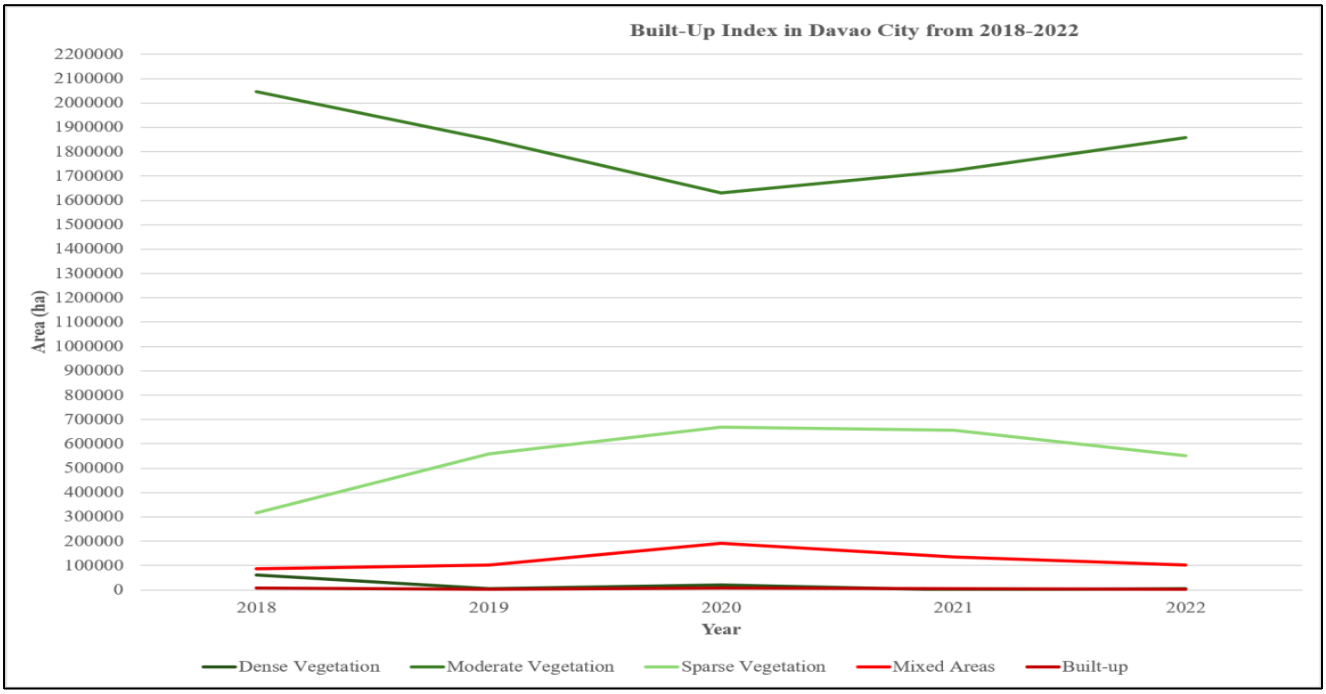

Fig 6 Graph Showing the Urban Expansion of Davao City from 2018-2022

Likewise, mixed areas increased from 87,568.22 ha (3.47%) in 2018 to 191,636.16 ha (7.60%) in 2020, before declining to 101,996.87 ha in 2022. The limited human activities during COVID-19 create temporary opportunities for ecosystem recovery and improved environmental quality (Bates et al., 2020) across terrestrial ecosystems (Diffenbaugh et al., 2020), such as lower pollution levels (Rume & Islam, 2020; Bates et al., 2020), restrictions on vehicles used, and industrial operations (Corlett et al., 2020) and anthropogenic pressures (Bashir et al., 2020).

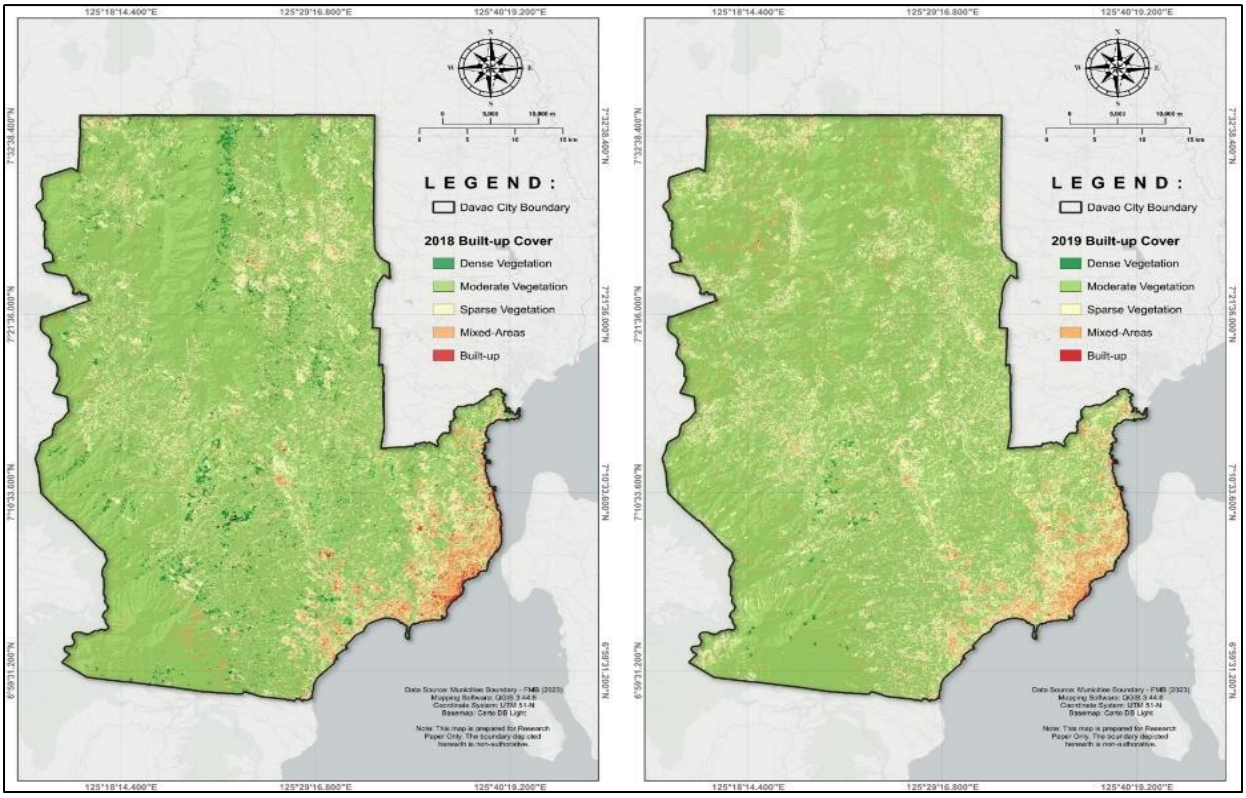

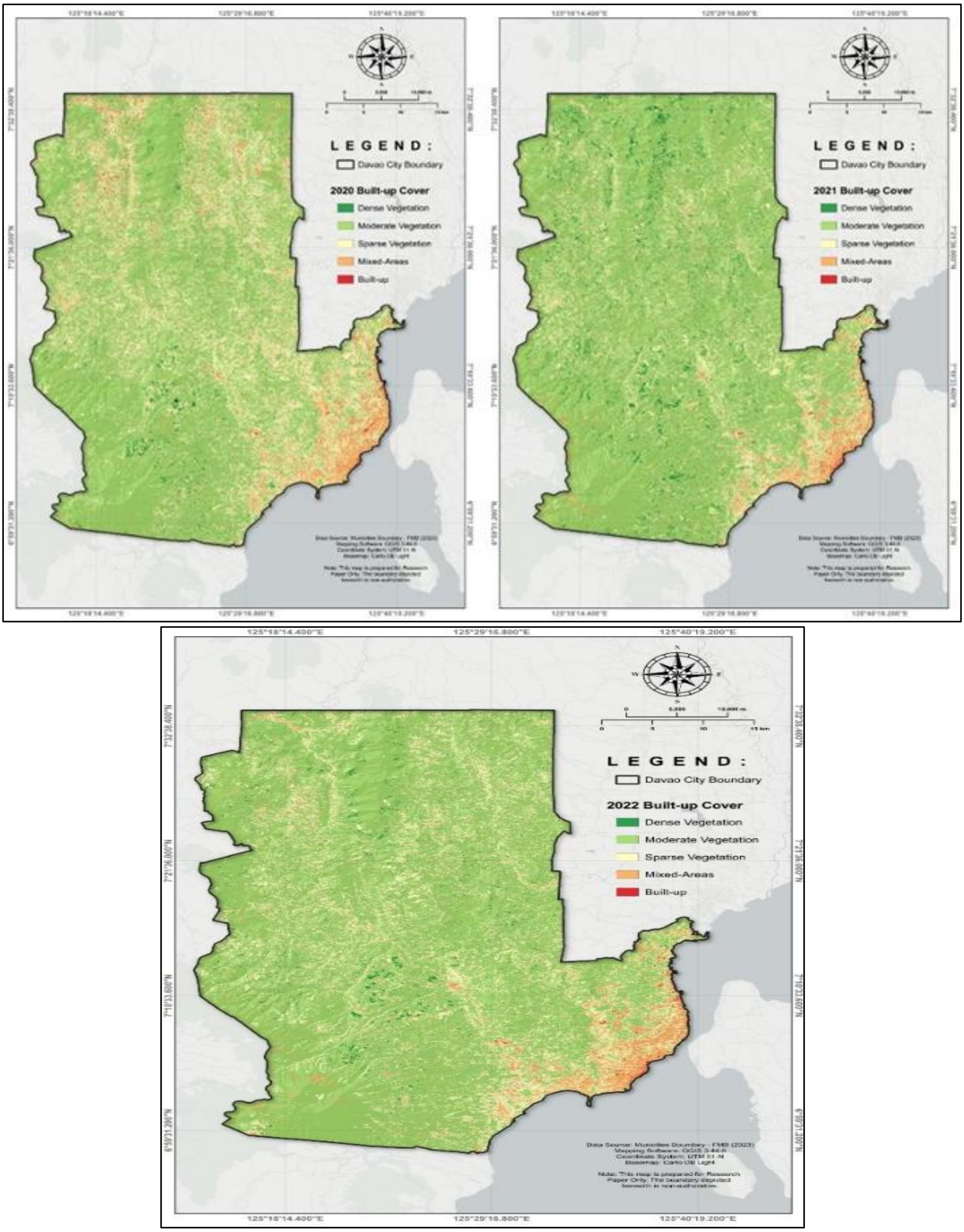

Fig 7 Spatio-Temporal Change in Urban Expansion in Davao City from 2018-202

➢ *Land Surface Temperature of Davao City from 2018 to 2022*

Table 5 and Figures 10 and 11 present the analysis of land surface temperatures in Davao City from 2018 to 2022. The data show considerable temporal variation in the thermal characteristics of the study area from 2018 to 2022, from very low to very high temperatures. In 2018, the study area exhibited very high temperatures of 28.70°C and very low temperatures of 5.40°C, indicating relatively cooler surface conditions that may be attributed to the abundance of vegetation and water bodies that mitigate surface heating by providing shade and facilitating evapotranspiration (Weng et al., 2004; Voogt & Oke, 2003).

ISSN No:-2456-2165 https://doi.org/10.38124/ijisrt/26jul851

Table 5 Land Surface Temperature of Davao City from 2018 -2022

YEAR	**Land Surface Temperature (°C)**	
	Very Low	Very High
2018	5.4	28.7
2019	11.01	33.32
2020	4.79	36.66
2021	9.38	33.2
2022	6.54	32.71

In 2019, both the very low 11.01°C and very high 33.32°C temperatures increased, reflecting an increase in surface temperature which may be associated with annual climatic fluctuations and localized alterations in land cover characteristics (Amiri et al., 2009).

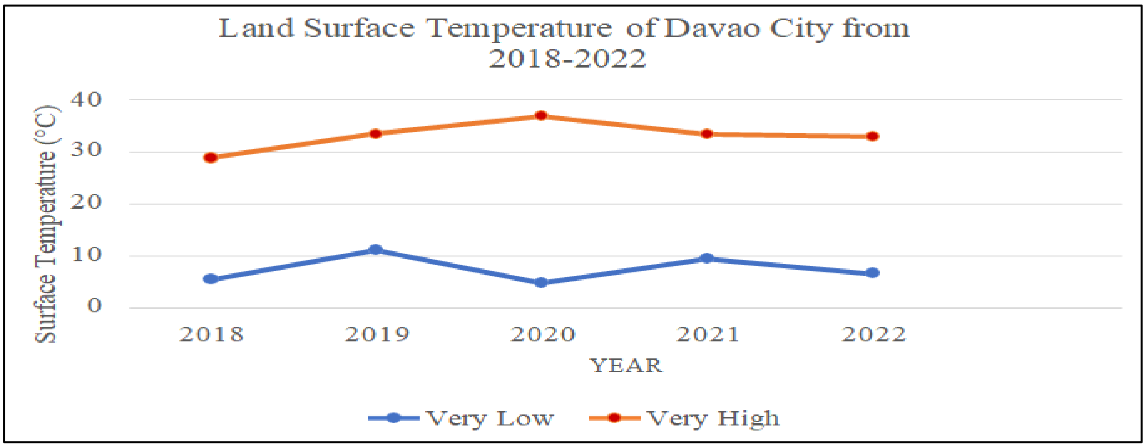

Fig 8 Graph Showing the Land Surface Temperature of Davao City from 2018-2022

The highest temperature of 36.66°C was recorded in 2020, while the very low temperature decreased to 4.79°C; the observed pattern is likely associated with the expansion of impervious surfaces, reduced vegetation density, and variations in annual meteorological conditions, collectively contributing to higher land surface temperature (Weng, 2009; Li et al., 2013). However, in 2021, a sudden decrease in the very high temperature was observed to 33. 20°C, whereas the very low temperature was increased to 9.38°C, this may indicate the combined influence of improved vegetation conditions. (Rasul et al., 2017). By 2022, the very high temperature further declined to 32.71°C with a very low temperature of 6.54°C.

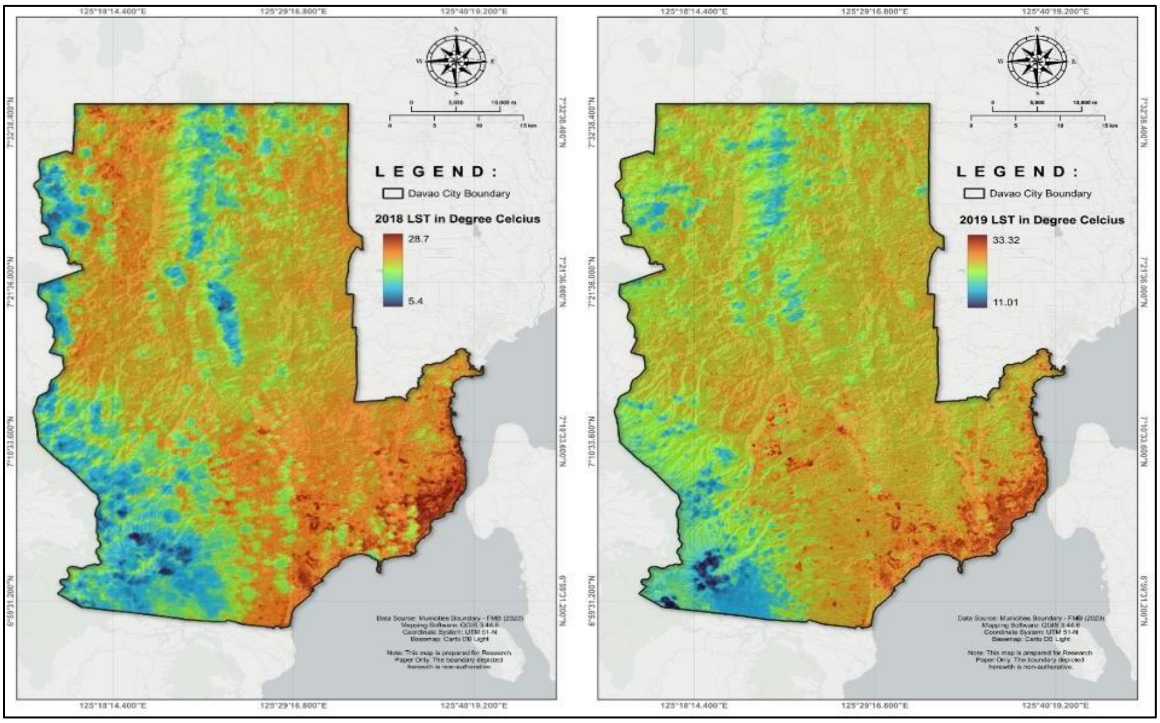

ISSN No:-2456-2165 https://doi.org/10.38124/ijisrt/26jul851

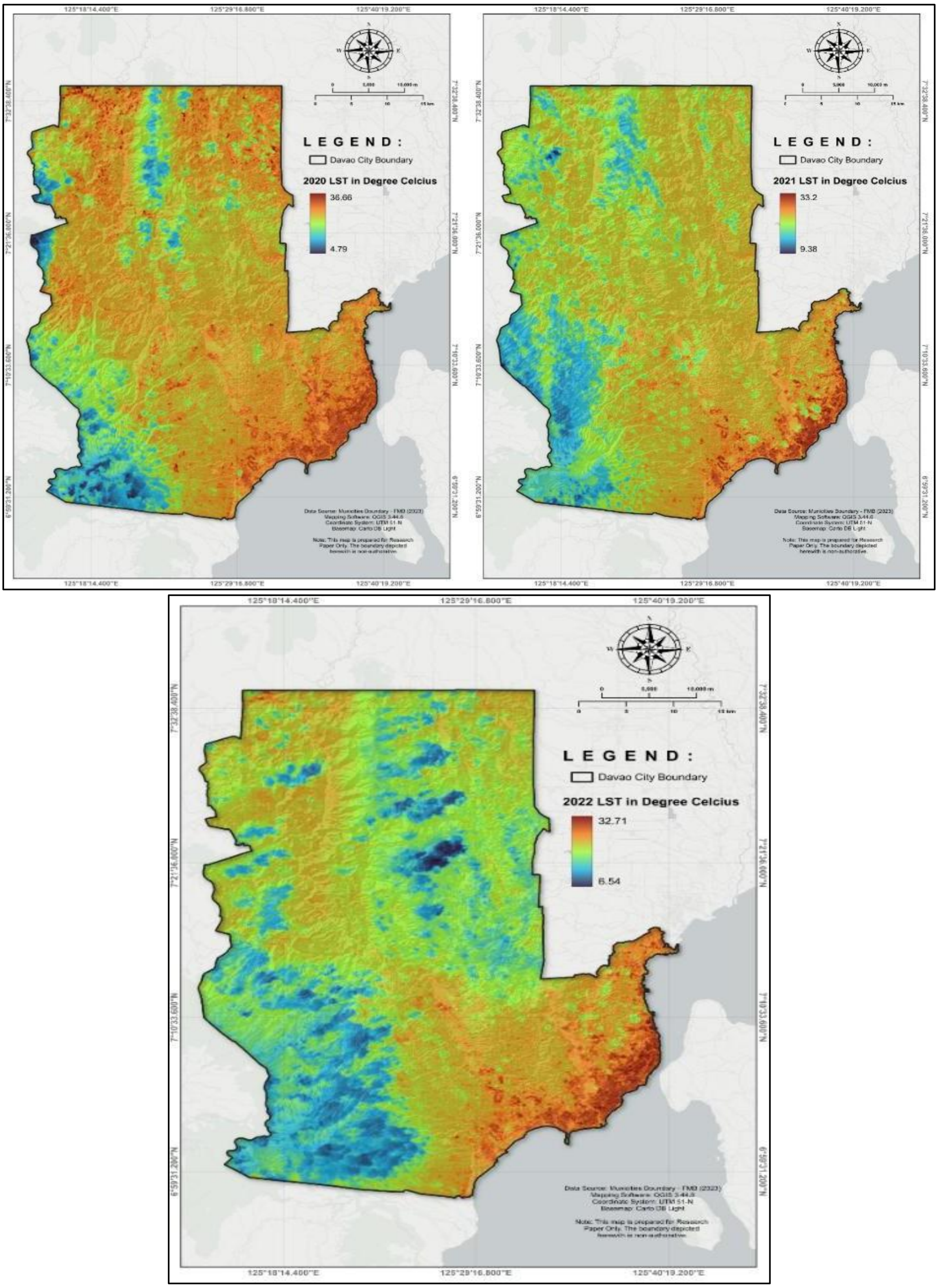

Fig 9 Spatio-Temporal Change in Land Surface Temperature of Davao City from 2018-2022

➢ *Correlation Analysis between NDVI, NDBI, and LST*

Table 6 Correlation Analysis between NDVI, NDBI, LST, and AADT

	NDBI	*NDVI*	*LST*
NDBI	1		
NDVI	-0.4313	1	
LST	0.621584	-0.24949	1

ISSN No:-2456-2165 https://doi.org/10.38124/ijisrt/26jul851

Table 6 shows that the correlation between NDBI and NDVI is moderate and negative (r = -0.4313), indicating that as built-up areas increase, vegetation cover decreases. This is expected in urbanizing environments where infrastructure expansion often replaces vegetated surfaces. In contrast, NDBI and LST showed a strong positive relationship (r = 0.621584), indicating that highly built-up areas tend to experience higher surface temperatures. Built-up materials such as concrete and asphalt absorb and retain heat, contributing to the urban heat island effect. This suggests that urban development significantly influences temperature variation within the study area. Lastly, the relationship between NDVI and LST showed a weak negative correlation (r = -0.24949), indicating that areas with higher vegetation cover generally experience lower temperatures. Vegetation helps regulate temperature through shading and evapotranspiration, although the weak relationship suggests that other environmental and anthropogenic factors also affect land surface temperature.

➢ *Policy Implications*

Based on the study's findings, policy implications include strengthening transportation planning through improved traffic signal systems, road widening projects, alternate routes, and enhanced public transportation services within major urban corridors. Implement roadside tree planting programs, preserve urban green spaces, and protect agricultural lands from unnecessary development. Promote sustainable transportation systems, such as modernized public utility vehicles, bike lanes, pedestrian-friendly infrastructure, and stricter vehicle-emission monitoring programs.

Integrate green infrastructure such as urban parks, rain gardens, green roofs, and permeable pavements into city planning and infrastructure development projects. Expand urban forestry and watershed protection programs, strengthen conservation initiatives in upland areas, and encourage community-based tree planting and sustainable landscape management.

IV. CONCLUSIONS & RECOMMENDATIONS

Thus, the study reveals that from 2018-2022; in terms of the vegetation index the moderate vegetation holds the highest area coverage from the aforementioned years this signifies that in terms of vegetation agricultural areas holds the highest coverage in the study area, there are times that the total area fluctuates due to the fact that during the capture of data in the landsat 8 coincides the date of pre or post-harvest of the farmers, second the built up index also fluctuates from 2018-2022 this variations due to the changes in the land cover types in where some changes may due to the effect of pandemic which hinders the continues expansion and the practices made by humans such a planting. Third, land surface temperature increases in built-up areas as built-up expansion occurs, whereas very low land surface temperatures are observed in areas with thick, healthy vegetation, which occupies a small land cover area. Fourth, in terms of traffic density, the barangay of Matina and the Davao City International Airport have the highest annual average traffic density across the five major roads. This suggests that almost all people traveled from the south to the north area. This is due to work-related reasons, schools, hospitals, malls, and the Davao airport. The correlation between NDBI and NDVI is negative, indicating that as built-up areas increase, vegetation decreases due to the conversion of vegetated areas to urban areas for infrastructure expansion. Conversely, the NDBI and LST presents a strong positive relationship which indicates that highly built-up areas hold the highest land surface temperature, Lastly, the NDVI and LST present a weak negative correlation emphasizes that areas with highest vegetation cover generally has the lowest land surface temperature. Overall, the results highlight the interconnected influence of urbanization, transportation activities, vegetation dynamics, and thermal conditions within the study area.

➢ *Recommendations*

Based on the findings of the study, it is recommended that the following:

- To Local Planners and Policymakers: To strengthen the integration of green infrastructure, particularly along major road networks, to help mitigate increasing land surface temperatures. The establishment of roadside tree planting, urban green buffers, and expanded green spaces is encouraged to reduce heat accumulation in areas with high traffic volume. In addition, land-use planning should be improved to better coordinate transportation development with urban expansion, minimizing fragmented landscapes and uncontrolled surface changes. Regular monitoring using remote sensing indicators such as NDVI, NDBI, and LST is also recommended to track environmental changes and guide evidence-based decision-making.
- Future Researchers: Should incorporate additional factors such as air quality, population growth, and seasonal climate variations to provide a more comprehensive understanding of urban heat dynamics in the city, and also better choose from the present years.

REFERENCES

[1]. Abdullah, M., Ali, N., Dias, C., et al. (2022). Exploring the impacts of COVID-19 on travel behavior and mode preferences. Transportation Research Interdisciplinary Perspectives, 13, 100540. https://doi.org/10.1016/j.trip.2021.100540

[2]. Acioly Jr., C & Payot, J. (2005). Process Mapping: Davao: building channels of participation and the land question Final.https://www.cordaid.org/nl/wpcontent/uploads/sites/2/2014/08/PM_Dav ao_Philippines_1.pdf

[3]. Afrin, T., & Yodo, N., (2020). A Survey of Road Traffic Congestion Measures towards a Sustainable and Resilient Transportation System. Sustainability. 12(11). 2:23. https://doi.org/10.3390/su12114660. May 7, 2026

ISSN No:-2456-2165 https://doi.org/10.38124/ijisrt/26jul851

[4]. A.K. Jebur. Uses and applications of geographic information systems Saudi J. Civ. Eng, 5 (2021), pp. 18-25. May 7, 2026

[5]. Akpoti, K. & Ofosu, E. & Kabo-bah, A. (2016). Impacts of Rainfall Variability, Land Use and Land Cover Change on Stream Flow of the Black Volta Basin, West Africa. Hydrology. 3. 26. 10.3390/hydrology3030026 May 7, 2026

[6]. Aloi, A., et al. (2020). Effects of the COVID-19 Lockdown on Urban Mobility: Empirical Evidence from the City of Santander (Spain). Sustainability, 12(9), 3870. https://doi.org/10.3390/su12093870

[7]. Amiri, R., Weng, Q., Alimohammadi, A., & Alavipanah, S. K. (2009). Spatial–temporal dynamics of land surface temperature in relation to fractional vegetation cover and land use/cover in the Tabriz urban area, Iran. Remote Sensing of Environment, 113(12), 2606–2617. https://doi.org/10.1016/j.rse.2009.07.021

[8]. Aronson, M. F. J., Lepczyk, C. A., Evans, K. L., Goddard, M. A., Lerman, S. B., MacIvor, J. S., Nilon, C. H., & Vargo, T. (2017). *Biodiversity in the city: Key challenges for urban green space management*. Frontiers in Ecology and the Environment, 15(4), 189–196.

[9]. Awotwi, A., Yeboah, F., & Kumi, M., (2015). Assessing the impact of land cover changes on water balance components of White Volta Basin in West Africa. Wiley online library https://doi.org/10.1111/wej.12100 May 7, 2026

[10]. Bashir, M. F., Ma, B., Bilal, Komal, B., Bashir, M. A., Tan, D., & Bashir, M. (2020).

[11]. Correlation between environmental pollution indicators and COVID-19 pandemic: A brief study in Californian context. Environmental Research, 187, 109652. https://doi.org/10.1016/j.envres.2020.109652

[12]. Bates, A. E., Primack, R. B., Moraga, P., & Duarte, C. M. (2020). COVID-19 pandemic and associated lockdown as a "Global Human Confinement Experiment" to investigate biodiversity conservation. Biological Conservation, 248, 108665. https://doi.org/10.1016/j.biocon.2020.108665

[13]. Bertinelli, L., & Black, D. (2004). Urbanization and growth. Journal of Urban Economics, 56(1), 80–96. https://doi.org/10.1016/j.jue.2004.03.003 May 7, 2026

[14]. Bucsky, P. (2020). Modal share changes due to COVID-19: The case of Budapest. Transportation Research Interdisciplinary Perspectives, 8, 100141. https://doi.org/10.1016/j.trip.2020.100141

[15]. Buyantuyev, A., & Wu, J. (2010). Urban heat islands and landscape heterogeneity: Linking spatiotemporal variations in surface temperatures to land-cover and socioeconomic patterns. Landscape Ecology May 7, 2026

[16]. Cabrera, J., & Dumadaya, C., (2023). Determination of future land use changes using remote sensing imagery and artificial neural network algorithm: A case study of Davao City, Philippines. Artificial Intelligence in Geosciences Volume 4, Pages 111-118.

[17]. Corlett, R. T., Primack, R. B., Devictor, V., Maas, B., Goswami, V. R., Bates, A. E., Koh, L. P., Regan, T. J., Loyola, R., Pakeman, R. J., Cumming, G. S., Pidgeon, A., Johns, D., & Roth, R. (2020). *Impacts of the coronavirus pandemic on biodiversity conservation*. Biological Conservation, 246, 108571. https://doi.org/10.1016/j.biocon.2020.108571

[18]. Chakraborty, T., & Maity, I. (2020). COVID-19 outbreak: Migration, effects on society, global environment and prevention. Science of the Total Environment, 728, 138882. https://doi.org/10.1016/j.scitotenv. 2020.138882 on May 7, 2026

[19]. Chen K, Wolf K, Breitner S, et al., (2018) UF &HEALTH Study Group. Two-way effect modifications of air pollution and air temperature on total natural and cardiovascular mortality in eight European urban areas. Environ Int 2018; 116:186-96. 10.1016/j.envint.2018.04. 021. May 7, 2026

[20]. Chang, Y. S., Jo, S. J., Lee, Y.-T., & Lee, Y. (2021). Population Density or Populations Size. Which Factor Determines Urban Traffic Congestion? Sustainability, 13(8), 4280. https://doi.org/10.3390/su13084280

[21]. Chowdhury et al, (2020). Land use/land cover change assessment of Halda watershed using remote sensing and GIS. Science direct. https://www.sciencedirect.com/science/article/pii/S1110982318300140#bb010 May 7, 2026

[22]. Diffenbaugh, N. S., Field, C. B., Appel, E. A., Azevedo, I. L., Baldocchi, D. D., Burke, M., Burney, J. A., Ciais, P., Davis, S. J., Fiore, A. M., Fletcher, S. M., Hertel, T. W., Horton, D. E., Hsiang, S. M., Jackson, R. B., Jin, X., Levi, M., Lobell, D. B., McKinley, G. A., ... Weber, C. L. (2020). *The COVID-19 lockdowns: A window into the Earth System*. Nature Reviews Earth & Environment, 1, 470–481. https://doi.org/10.1038/s43017-020-0079-1

[23]. D'Odorico, P. & Sujith, R. (2016). Land Degradation and Environmental Challenge. Science direct. https://doi.org/10.1016/B978-0-12-394847- 2.00014-0 Domingo, S., & Manejar, A. J., (2018). Forest Protection in the Philippines. https://pidswebs.pids.gov.ph/CDN/PUBLICATIONS/pidsdps1853.pdf on May 7, 2026

[24]. Fenta A, Yasuda H, and Shimizu K, et al. (2017). Spatial distribution and temporal trends of rainfall and erosivity. In the Eastern Africa region. Hydrological Processes. 2017; 31:4555 4567.https://doi.org/10.1002/hyp.11378

[25]. Foley, J. A., et al. (2005). Global consequences of land use. Science, 309(5734), 570–574. DOI: https://doi.org/10.1126/science.1111772

[26]. Fu, X. P., Mou, B., & Griffy-Brown, C. The combination of digital technology and architectural design to develop a process for enhancing energy-saving: The case of Maanshan China. Technology in Society, 2014, 39, 77-87. May 7, 2026

[27]. Gallivan, S., & Heydecker, b., (1988). Optimising the

control performance of traffic signals at a single junction. Transportation Research Part B: Methodological. 22:5, 357:370. https://doi.org/10.1016/0191-2615(88)90040-9

[28]. Ghandi, U., (2023). Creating Heatmaps. Accessed from https://www.qgistutorials.com/en/docs/creating_heatmaps.html on December 7, 2024

[29]. Gessesse B, Bewket W, and Bräuning A (2015) Model-based characterization and monitoring of runoff and soil erosion in response to land use/cover changes in the Modjo watershed, Ethiopia. Land Degrad Dev 26:711-724.https://environmentalsystemsresearch.springeropen.com/articles/10.1186/s 40068-019-0148-y on May 7, 2026

[30]. Gong, P.; Liang, S.; Carlton, E.J.; Jiang, Q.; Wu, J.; Wang, L.; Remais, J.V. Urbanisation and health in China. Lancet 2012, 379, 843–852.

[31]. Grimm, N.B., Faeth, S.H., Golubiewski, N.E., Redman, C.L., Wu, J., Bai, X., et al., 2008. Global change and the ecology of cities. Science 319, 756–760. Accessed from https://sci-hub.se/https://doi.org/10.1016/j.scitotenv.2018.11.171on February 13, 2024

[32]. Grover, A., & Singh R. B., (2015). Analysis of Urban Heat Island (UHI) in Relation to Normalized Difference Vegetation Index (NDVI): A Comparative Study of Delhi and Mumbai.MDPI. Accessed from https://www.mdpi.com/20763298/2/2/125#B7-environments-02-00125on February 21, 2024

[33]. Hahn, E, Chatterjee, A, Younger, M. (2002). Macro-Level Analysis of factors related to Areawide highway traffic congestion.Transportation Research Record, Vol. 1817, p. 11-16. https://doi.org/10.3141/1817-02

[34]. Haines A, Ebi K. The imperative for climate action to protect health. N Engl J Med 2019; 380:263-73. 10.1056/NEJMra1807873

[35]. Hearne, D., Gamboa, R., & Monsanto, V. M. (2008). From ideas to action: A review of Implementing HELP principles in river basins with limited resources and capacity. Water SA, 34(4), 504–511. https://doi.org/10.4314/wsa.v34i4.183663

[36]. Hargrove, W. L., & Heyman, J. M. (2020). A comprehensive process for stakeholder identification and engagement in addressing wicked water resources problems. Land, 9(4), 119. https://doi.org/10.3390/land9040119

[37]. Imhoff, M.L., Zhang, P., Wolfe, R.E., Bounoua, L., 2010. Remote sensing of the urban heat island effect across biomes in the continental USA. Remote Sens. Environ. 114, 504–513. Accessed from https://scihub.se/https://doi.org/10.1016/j.scitotenv.2018.11.171on February 13, 2024

[38]. Jensen, J.R. (2015). Introductory Digital Image Processing: A Remote Sensing Perspective (4th Edi.). https://books.google.com.ph/books?id=BWx3CgAAQBAJ

[39]. Jiang, H., Ji, L., Yu, K., & Zhao, Y. (2024). *Analysis of the Substantial Growth of Water Bodies during the Urbanization Process Using Landsat Imagery—A Case Study of the Lixiahe Region, China*. Remote Sensing, 16(4), 711. https://doi.org/10.3390/rs16040711

[40]. Kuang, W.; Chi, W.; Lu, D.; Dou, Y. A comparative analysis of megacity expansions in China and the U.S.: Patterns, rates and driving forces. Landsc. Urban Plan. 2014, 132, 121–135. Accessed from https://www.mdpi.com/2076-3298/2/2/125#B7-environments-02-00125 on February 21, 2024

[41]. Kuddus, M.A., Tynan, E. & McBryde, E. (2020). Urbanization: a problem for the rich and the poor?. Public Health Rev 41, 1.https://doi.org/10.1186/s40985-0190116-0

[42]. Lai, L., Huang, X., Yang, H., Chuai, X., Zhang, M., Zhong, T., Chen, Z., Chen, Y., Wang, X., & Thompson, J. R. (2016). Carbon emissions from land use change and management in China between 1990 and 2010. Science Advances, 2(11), 1–9.https://agupubs.onlinelibrary.wiley.com/doi/full/10.1029/2018EF000932

[43]. Lambin, E. F., et al. (2001). The causes of land-use and land-cover change. Global Environmental Change, 11(4), 261–269. DOI: https://doi.org/10.1016/S0959-3780(01)00007-3

[44]. Li, Z. L., Tang, R., Wan, Z., Bi, Y., Zhou, C., Tang, B., Yan, G., & Zhang, X. (2013). *Satellite-derived land surface temperature: Current status and perspectives*. Remote Sensing of Environment, 131, 14–37. https://doi.org/10.1016/j.rse.2012.12.008

[45]. Liu, S., Hongbo, X., Li, W., Wang, L., Yang, H., & Liang (2016). Quantifying spatial-temporal pattern of urban heat island in Beijing: An improved assessment using land surface temperature (LST) time series observations from Landsat, MODIS, and Chinese new satellite GaoFen-1. IEEE Journal of Selected Topics in Applied Earth Observations and Remote Sensing, 9(5), 2028–2042. https://doi.org/10.1109/JSTARS.2015.2512545

[46]. Mao W, Wang X, Cai J, Zhu M. (2016). Multidimensional histogram-based information capacity analysis of urban heat island effect using Landsat 8 data. Remote Sensing Letters 7(10): 925-934. http://doi.org/10.1080/2150704X.2016.1182656

[47]. Ng, B. J. et al. (2015). Carbon fluxes from an urban tropical grassland. https://www.nature.com/articles/srep44049 on May 6, 2025

[48]. Perini, K., & Magliocco, A. (2014). Effects of vegetation, urban density, building height, and atmospheric conditions on local temperatures and thermal comfort. Urban Forestry & Urban Greening, 13(3), 495-506. DOI: https://doi.org/10.1016/j.ufug.2014.03.003

[49]. Pettorelli, N., Vik, J. O., Mysterud, A., Gaillard, J. M., Tucker, C. J., & Stenseth, N. C. (2005). Using the satellite-derived NDVI to assess ecological responses to environmental change. Trends in Ecology & Evolution, 20(9), 503–510.

https://doi.org/10.1016/j.tree.2005.05.011
[50]. Porio, E., (2022). Urban Poor Community Strategies: Towards a Resilient Recovery from Natural Disasters and the Covid-19 Pandemic in the Philippines. https://link.springer.com/chapter/10.1007/978-3-030-93695-2_12 on February 24, 2025
[51]. Ranjan, A. K., Patra, A. K., & Gorai, A. K. (2021). Effect of lockdown due to SARS COVID-19 on aerosol optical depth and land surface temperature in India. Environmental Challenges, 2, 100031.https://doi.org/10.1016/j.envc 2021.100031on May 7, 2026
[52]. Rashid, N., Alam, J. A. M. M., Chowdhury, M. A., & Islam, S. L. U. (2022). Impact of landuse change and urbanization on urban heat island effect in Narayanganj city, Bangladesh: A remote sensing-based estimation. Environmental Challenges. https://doi.org/10.1016/j.envc.2022.100571 on February 26, 2025
[53]. Rasul, A., Balzter, H., Smith, C., Remedios, J., Adamu, B., Sobrino, J. A., Srivanit, M., & Weng, Q. (2017). *A review on remote sensing of urban heat and cool islands*. Land, 6(2), 38. https://doi.org/10.3390/land6020038
[54]. Rawat and Kumar, (2015). Monitoring land use/cover change using remote sensing and GIS techniques: a case study of Hawalbagh block, district Almora, Uttarakhand, India. Science direct. https://www.sciencedirect.com/science/article/pii/S1110982318300140#bb0105 on March 26, 2025
[55]. Ray, S. (2011). Impact of Population Growth on Environmental Degradation: Case of Study. Journal of Economics and Sustainable Development. Vol.,2. https://core.ac.uk/download/pdf/234645493.pdf on March 15, 2025
[56]. Rume, T., & Islam, S. M. D.-U. (2020). Environmental effects of COVID-19 pandemic and potential strategies of sustainability. Heliyon, 6(9), e04965. https://doi.org/10.1016/j.heliyon.2020.e04965
[57]. S. Angel et al, (2011). The dimensions of global urban expansion: estimates and projections for all countries, 2000–2050. Retrieved from https://doi.org/10.1016/j.scitotenv.2015.11.168 on February 2, 2024
[58]. Shalaby, A. and R. Tateishi (2007). Remote sensing and GIS for mapping and monitoring land cover and land-use changes in the Northwestern coastal zone of Egypt, Appl Appl. Geogr., 27pp. 28-41, 10.1016/j.apgeog.2006.09.004 on February 2, 2024
[59]. Shakibaei, S., de Jong, G. C., Alpkökin, P., & Rashidi, T. H. (2021). Impact of the COVID-19 pandemic on travel behavior in Istanbul: A panel data analysis. Sustainable Cities and Society, 65, 102619. https://doi.org/10.1016/j.scs.2020.102619
[60]. Sharifi, A., & Khavarian-Garmsir, A. R. (2020). The COVID-19 pandemic: Impacts on cities and major lessons for urban planning, design, and management. The Science of the total environment, 749, 142391.https://doi.org/10.1016/j.scitotenv.2020.142391
[61]. Sun, Ge & Caldwell, Peter 2015. Impacts of urbanization on stream water quantity and quality in the United States. Water Resources Impact, Volume 17 Number 1. 4 p. Accessed from https://www.srs.fs.usda.gov/pubs/ on February 21, 2024
[62]. Sun, Q., Wu, Z. and Tan, J. (2012) The Relationship between Land Surface Temperature and Land Use/Land Cover in Guangzhou, China. Environmental Earth Sciences, 65, 1687-1694. http://dx.doi.org/10.1007/s12665-011-1145-2
[63]. Seto, K. C., et al. (2012). Global forecasts of urban expansion. PNAS, 109(40), 16083–16088.DOI: https://doi.org/10.1073/pnas.1211658109 on My 6, 2026
[64]. Seto, K. C., Güneralp, B., & Hutyra, L. R. (2012). *Global forecasts of urban expansion to 2030 and direct impacts on biodiversity and carbon pools*. Proceedings of the National Academy of Sciences, 109(40), 16083–16088. https://doi.org/10.1073/pnas.1211658109
[65]. Tewabe, D. & Fentahun, T. (2020). Assessing land use and land cover change detection using remote sensing in the Lake Tana Basin, Northwest Ethiopia. tandofline. Accessed from https://www.tandfonline.com/doi/pdf/10.1080/23311843.2020.177899 on February 21, 2024
[66]. Tong, S., Prior, J., McGregor. G., Shi. X., & Kinney, P., (2021). Urban heat: an increasing threat to global health. https://doi.org/10.1136/bmj.n2467
[67]. Tucker, C. J. (1979). Red and photographic infrared linear combinations for monitoring vegetation. Remote Sensing of Environment, 8(2), 127–150.https://doi.org/10.1016/0034-4257(79)90013-0 on February 16, 2025
[68]. Turner, B. L., et al. (2007). Land change science: Concepts and applications. Global EnvironmentalChange, 17(3–4), 321–322. DOI: https://doi.org/10.1016/j.gloenvcha.2007.07.005Oke, T. R. (1982). The energetic basis of the urban heat island. Quarterly Journal of the Royal Meteorological Society, 108(455), 1–24. on May 6, 2026
[69]. Van Dijk, A. I. et al. (2013). The Millennium Drought in southeast Australia (2001–2009): natural and human causes and implications for water resources, ecosystems. Econ. Soc. Water Resour. Res. 49, 1040–1057. https://doi.org/10.1038/s41467-022-31125-6 on May 5, 2026
[70]. Voogt, J. A., & Oke, T. R. (2003). Thermal remote sensing of urban climates. Remote Sensing of Environment, 86(3), 370–384. https://doi.org/10.1016/S0034-4257(03)00079-8
[71]. United Nations, (2014). Department of Economic and Social Affairs, Population Division. World urbanization prospects: The 2014 revision, New York: NY, United Nations 2014. Accessed doi.org/10.1016/j.scitotenv.2015. 11.168 from on February 4, 2024
[72]. Ursu, C. (2019). The Land Surface Temperature Evolution (LST) using Landsat Scenes. Case Study:

The Industrial Platform Săvinești. Geographia Technica, 14(2), 131–142. https://doi.org/10.21163/GT_2019. 142.12 on February 24, 2025

[73]. Weng, Q. (2012). Remote sensing of impervious surfaces in urban areas: Requirements, methods, and trends. Remote Sensing of Environment, 117,34–49. https://doi.org/10.1016/j.rse.2011. 02.030 on March 6, 2026

[74]. Weng, Q. (2009). Thermal infrared remote sensing for urban climate and environmental studies: Methods, applications, and trends. ISPRS Journal of Photogrammetry and Remote Sensing, 64(4), 335–344. https://doi.org/10.1016/j.isprsjprs.2009.03.007

[75]. Weng, Q., Lu, D., & Schubring, J. (2004). Estimation of land surface temperature–vegetation abundance relationship for urban heat island studies. Remote Sensing of Environment, 89(4), 467–483. https://doi.org/10.1016/j.rse.2003.11.005

[76]. Wang, Mingshu & Debbage, Niel (2022). Urban morphology and traffic congestion: Longitudinal evidence from US cities, Computers, Environment and Urban Systems, Volume 89, 2021, 101676, ISSN 0198-9715, https://doi.org/10.1016/j.compenvurbsys.2021.101676.

[77]. Wu Q., Li H.Q., Wang R.S., Paulussen J., He H., Wang M., Wang B.H., Wang Z., (2006). Monitoring and predicting land use change in Beijing using remote sensing and GIS. NCBI. https://www.ncbi.nlm.nih.gov/pmc/articles/PMC3707445/#b23-sensors-0806188 on February 26, 2025

[78]. Yao, R., Wang, L., Huang, X., Guo, X., Niu, Z., Liu, H., (2017). Investigation of urbanization effects on land surface phenology in Northeast China during 2001–2015. Remote Sens. 9, 66–81. Retrieved from doi: 10.1016/j.scitotenv.2018.11.1 on February 2, 2024

[79]. Zha, Y., Gao, J., and Ni, S., (2003). Use of the Abdullah, M., Ali, N., Dias, C., et al. (2022). Exploring the impacts of COVID-19 on travel behavior and mode preferences. Transportation Research Interdisciplinary Perspectives, 13, 100540. https://doi.org/10.1016/j.trip.2021.100540 normalized difference built-up index in automatically mapping urban areas from TM imagery. International Journal of Remote Sensing, 24(3), 583-594. https://doi.org/10.1080/01431160304987